

Compact TLS scanners in engineering: potential for monitoring deformations of tall structures

Kinga Wawrzyniak¹, ✉

Agnieszka Łańduch¹

¹ Faculty of Geoengineering, Mining and Geology, Wrocław University of Science and Technology

✉ Corresponding author: kinga.wawrzyniak@pwr.edu.pl

Summary

This study investigates the applicability of a compact terrestrial laser scanner (Leica BLK360) for assessing the verticality of a tall industrial chimney, and compares its performance with high-precision total station measurements. In the first phase, a reference control network was established and observed using the tangential envelope method with a total station, providing a precise benchmark. Terrestrial laser scanning was then carried out, and circles were fitted to horizontal cross-sections extracted from the point cloud. A least-squares approach was used to calculate chimney-axis deviations and evaluate verticality along the height of the structure. The results of both methods revealed a consistent trend of deviations increasing with height. Maximum differences between the total station and TLS measurements did not exceed 5 mm, which remains within acceptable geodetic tolerance. This demonstrates that the BLK360 is capable of providing sufficiently accurate data for preliminary deformation monitoring of tall engineering structures. The main advantage of the BLK360 scanner lies in its rapid and automated data acquisition, which allows for more frequent observations, reduced fieldwork time, and early detection of structural irregularities. However, limitations such as a reduced measurement range, lower sensitivity under unfavorable conditions, and dependency on surface reflectivity were also identified. Despite these constraints, the study confirms that the BLK360 can serve as a valuable supplementary tool to conventional total station surveys, offering practical support for ongoing monitoring, and contributing to improved safety in engineering practice.

Keywords

industrial chimney • verticality measurement • total station measurement • terrestrial laser scanning

1. Introduction

Slender engineering structures, such as industrial chimneys, cooling towers, masts, and telecommunication towers, represent a significant area of research within engineering geodesy and structural health monitoring [Gikas 2012]. Owing to their considerable height, susceptibility to dynamic influences, and operational importance, these structures are the focus of numerous studies that apply both conventional and advanced measurement techniques.

Classical geodetic methods, such as total station (TS) measurements, provide high, millimetre-level accuracy; however, their implementation requires precise instrumentation, is time-consuming, and remains prone to observer-related errors [Głowacki 2022]. An alternative is the use of GNSS measurements, which can also ensure high accuracy but require access to appropriate measurement infrastructure, thereby increasing the overall cost of surveys [Chmielewski et al. 2009]. In recent years, terrestrial laser scanning (TLS) has been increasingly employed [Beshr et al. 2023, Marjetič 2018, Siwiec and Lenda 2022], enabling rapid, automated, and contactless acquisition of spatial data with high point density and millimetre-level accuracy [Barazzetti et al. 2019, Teng et al. 2022]. Scanning an object allows for the collection of a significantly larger number of points compared to any total station survey [Matwij et al. 2024]. Nevertheless, total station remains essential for establishing control points, which facilitates the registration of TLS point clouds and enables quality assessment of the registration. Ensuring stable control points in the vicinity of the object is crucial, as it guarantees the repeatability of measurements over time [Barazzetti et al. 2019].

In the literature, several strategies for TLS data analysis used to assess the verticality and deformation of slender structures have been distinguished. The first approach is the cross-sectional method, in which circles are fitted to thin layers of the point cloud at different heights, allowing for the determination of the structural axis displacement and the evaluation of its deviation from verticality [Marjetič and Štebe 2017, Matwij et al. 2024, Muszynski and Milczarek 2017]. The second approach involves parametric surface modeling, enabling the direct determination of the inclination angle of the structural axis, as well as more advanced analysis of geometric deformations, such as ovalization or irregularities of walls. This approach is mainly applied when the shape of the object is somewhat more complex, e.g., in the case of cooling towers or wind turbine blades [Muszynski and Milczarek 2017, Pleterski et al. 2024, Popović et al. 2022]. Another method is the projection of surface point coordinates onto a vertical plane, used, for example, in the analysis of cooling towers, which allows for determining the wall curvature equation, calculating the axis inclination, and identifying local deformations [Beshr et al. 2023]. The integration of TLS data with other technologies, including photogrammetry and radar interferometry [Owerko et al. 2012], enables a comprehensive assessment of the structural condition [Daliga and Kurałowicz 2019, Zrinjski et al. 2021].

Previous studies indicate that TLS measurements are primarily performed using advanced, high-precision geodetic scanners. In practice, however, there may be

a need to use simpler, more affordable, and more mobile instruments, whose measurement capabilities have not yet been extensively analyzed. In this study, an attempt was made to verify the applicability of the Leica BLK360 compact scanner – a device with limited range and lower accuracy compared to standard geodetic instruments – for the measurement of slender structures. The aim of the study is to evaluate the suitability of a lower-class scanner for basic analyses of the geometry of slender constructions. Deviations from the verticality of the chimney axis obtained from TLS measurements were calculated by fitting circles at each analyzed level, and then compared with total station measurements and computations using the tangential envelope method.

2. Materials and methods

The object of the survey is a brick industrial chimney, currently out of service, located next to the historic Water Tower on Na Grobli Street in Wrocław. The height of the chimney, including its base, is 42 meters.

2.1. Methods

The research approach involves comparing the results of determining the verticality of the chimney using two measurement methods: total station and terrestrial laser scanning. Measurements were conducted simultaneously under stable weather conditions: temperature 21°C, pressure 1019 hPa, wind speed 10 m/s. The reference instrument was a Trimble C5 electronic total station, with an angular measurement accuracy of 15'' and a distance measurement accuracy of 2 mm + 2 ppm. The Leica Geosystems BLK360 scanner, on the other hand, features an integrated fast HDR spherical imaging system. Scans were performed panoramically with a vertical scanning range of 270°, a maximum range of 45 meters, and a scanning speed of 680,000 points per second. The control points P1–P5 and the surveyed targets T1–T10 are shown in Figure 1.

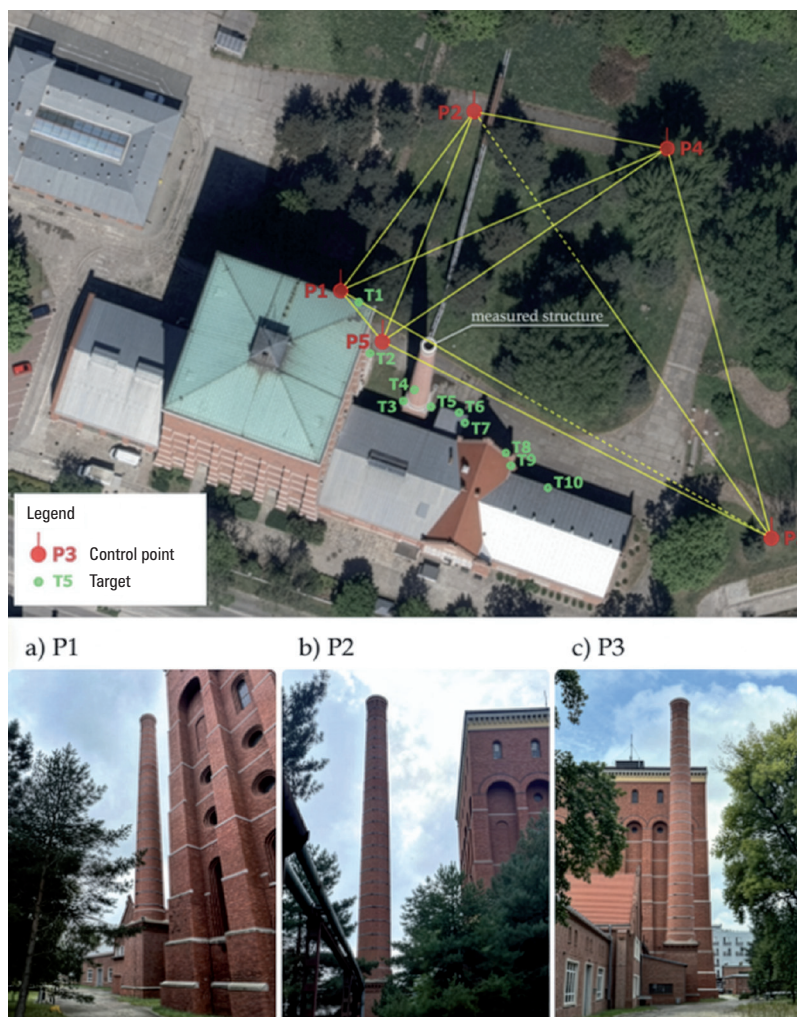
2.1.1. Total station

For the chimney verticality measurements using the total station, the tangential envelope method was employed. Initially, the reference network points P1–P5 (Fig. 1) were stabilized, after which they were measured with a total station in two series from two different telescope orientations.

The control points were additionally measured using GNSS in order to determine the cardinal directions. Subsequently, the verticality survey was carried out simultaneously from three stations: P1, P2, and P3. Measurements of the left and right tangents were performed at eight characteristic levels of the chimney 0–7 (Fig. 2).

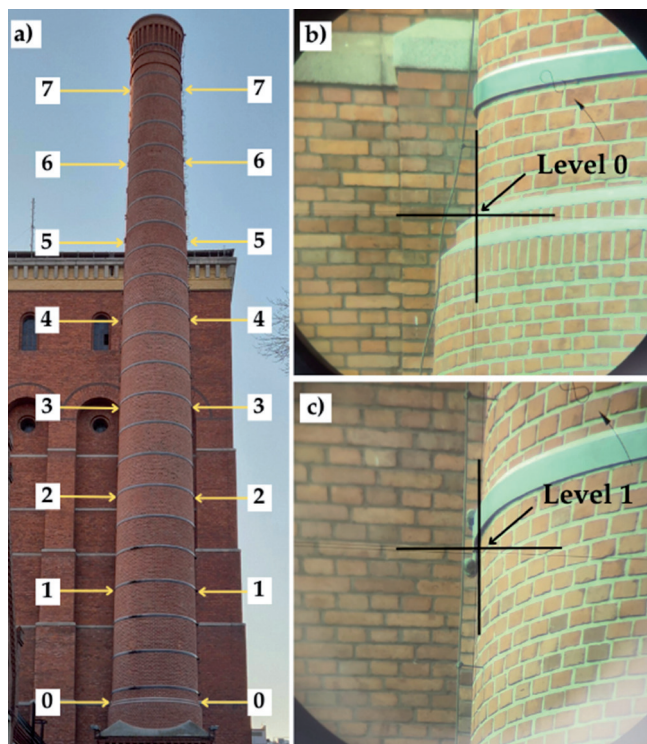
The control points were adjusted using the least squares method in the C-GEO software. During the free-network horizontal adjustment, point P4 was determined with the lowest accuracy, with an error of 2 mm, while the mean square positional error was

1.5 mm. In the vertical adjustment, the least accurate point was P3, with an error of 1.1 mm. Subsequently, the coordinate system was transformed so that its origin was placed at the center of the chimney at level 0, while preserving the cardinal directions. The mean discrepancy in horizontal angle observations during tangent measurements was $20''$ ($\approx 0.6''$ of arc). The mean direction of the chimney axis was calculated for each level and instrument station, followed by determining the angular deviations relative to level 0. Finally, differential adjustments were performed in C-GEO, yielding the chimney axis displacements at individual levels in the X and Y directions.



Source: Authors' own study

Fig. 1. Reference network with sightlines from control points a) P1, b) P2, c) P3



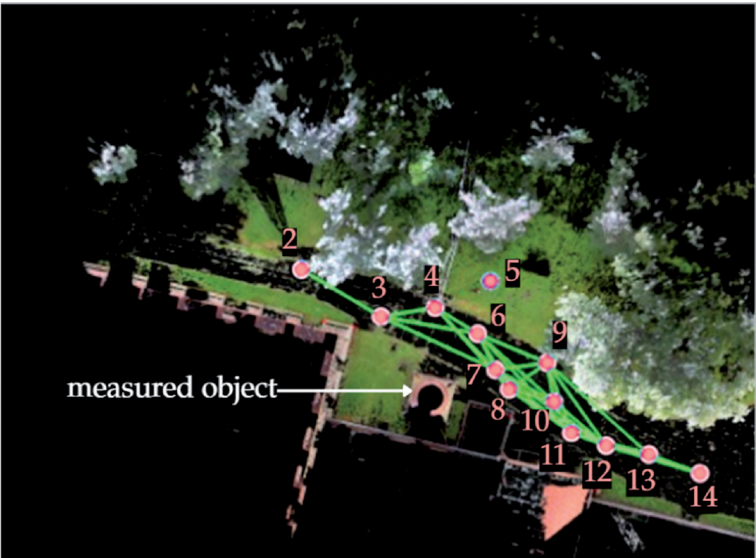
Source: Authors' own study

Fig. 2. Characteristic levels of the chimney (a) with the method of targeting level 0 (b) and each subsequent level (c)

2.1.2. Terrestrial Laser Scanning

The chimney was scanned from 14 stations (Fig. 3). Ten targets dedicated for Leica scanners, each with a diameter of 10 cm, were affixed to the structure and its immediate surroundings. The centers of the targets, as well as characteristic edges on the chimney, were measured with a Trimble C5 total station in order to provide georeferencing (a coordinate system consistent with that used in the method of surrounding tangents).

The registrations were performed in Cyclone Register 360 PLUS. Unfortunately, despite scanning the targets from a maximum distance of 12–15 meters, they were not detected by the software and were therefore not included in the registration process. Due to the scan density, 33 connections between scans were identified. The overlap amounted to 54%, and the strength to 74%. The connections detected between individual stations are shown in Figure 4. Two stations were excluded from the registration process because they were located too far from the previous stations, resulting in insufficient overlap that disrupted the registration.



Source: Authors' own study

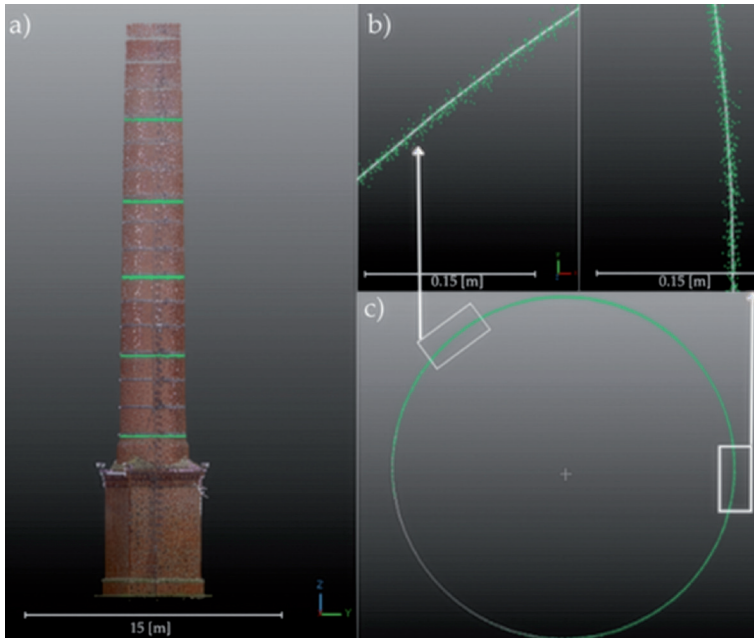
Fig. 3. Scanner stations during the survey of the structure

| | S11 | S12 | S8 | S10 | S9 | S13 | S14 | S7 | S6 | S3 | S4 | S2 |
|-----|-----|-----|----|-----|----|-----|-----|----|----|----|----|----|
| S11 | | | | | | | | | | | | |
| S12 | | | | | | | | | | | | |
| S8 | | | | | | | | | | | | |
| S10 | | | | | | | | | | | | |
| S9 | | | | | | | | | | | | |
| S13 | | | | | | | | | | | | |
| S14 | | | | | | | | | | | | |
| S7 | | | | | | | | | | | | |
| S6 | | | | | | | | | | | | |
| S3 | | | | | | | | | | | | |
| S4 | | | | | | | | | | | | |
| S2 | | | | | | | | | | | | |

Source: Authors' own study

Fig. 4. Connections detected between individual scanner stations

Georeferencing was performed in CloudCompare by selecting characteristic points and edges on the point cloud that had been previously measured with a total station. Cross-sections of the point cloud were then extracted at the heights of the levels measured with a total station. Although the chimney height was within the device's declared scanning range and the measurement stations were located in the immediate vicinity of the structure, only five of the eight measurement levels could be extracted. The Fit-Circle tool was subsequently applied to the cross-sections to fit a circle and determine their centers and radius (Fig. 5).



Source: Authors' own study

Fig. 5. Circle fitting in a point cloud: (a) view of the extracted chimney levels, (b) detailed view of the point cloud with the fitted circle, (c) circle fitting for level 2

A circle is fitted to a selected subset of the point cloud. The procedure begins with determining the best-fit plane by means of principal component analysis, followed by projecting the points onto this plane. In the resulting 2D coordinate system, circle fitting is carried out using the least squares method, which minimizes the deviations of the data points from the geometric model. The equation takes the following form:

$$x^2 + y^2 + ax + bx + c = 0 \quad (1)$$

Accordingly, for each point (x_i, y_i) , the equation can be expressed in a linear form with respect to the unknown parameters a, b, c :

$$ax_i + by_i + c = -(x_i^2 + y_i^2) \quad (2)$$

Collecting the equations for all points yields a linear equation:

$$AX = L \quad (3)$$

where:

$$\begin{aligned} A &= [x_1 x_2 \dots x_n y_1 y_2 \dots y_n 1 1 \dots 1], \\ X &= [abc], \\ L &= [- (x_1^2 + y_1^2) - (x_2^2 + y_2^2) \dots - (x_n^2 + y_n^2)] \end{aligned} \quad (4)$$

The solution is obtained from the formula:

$$X = (A^T A)^{-1} A^T L \quad (5)$$

From the determined parameters the circle center coordinates and the radius are obtained:

$$x_0 = -\frac{a}{2}, \quad y_0 = -\frac{a}{2}, \quad (6)$$

$$r = \sqrt{x_0^2 + y_0^2 - c} \quad (7)$$

Given the calculated circle centers and radius, the root mean square (RMS) fitting error can be determined as follows:

$$RMS = \sqrt{\frac{1}{n} \sum_{i=1}^n \left(\sqrt{(x_i - x_0)^2 + (y_i - y_0)^2} - r \right)^2} \quad (8)$$

where n – number of points in the selected subset.

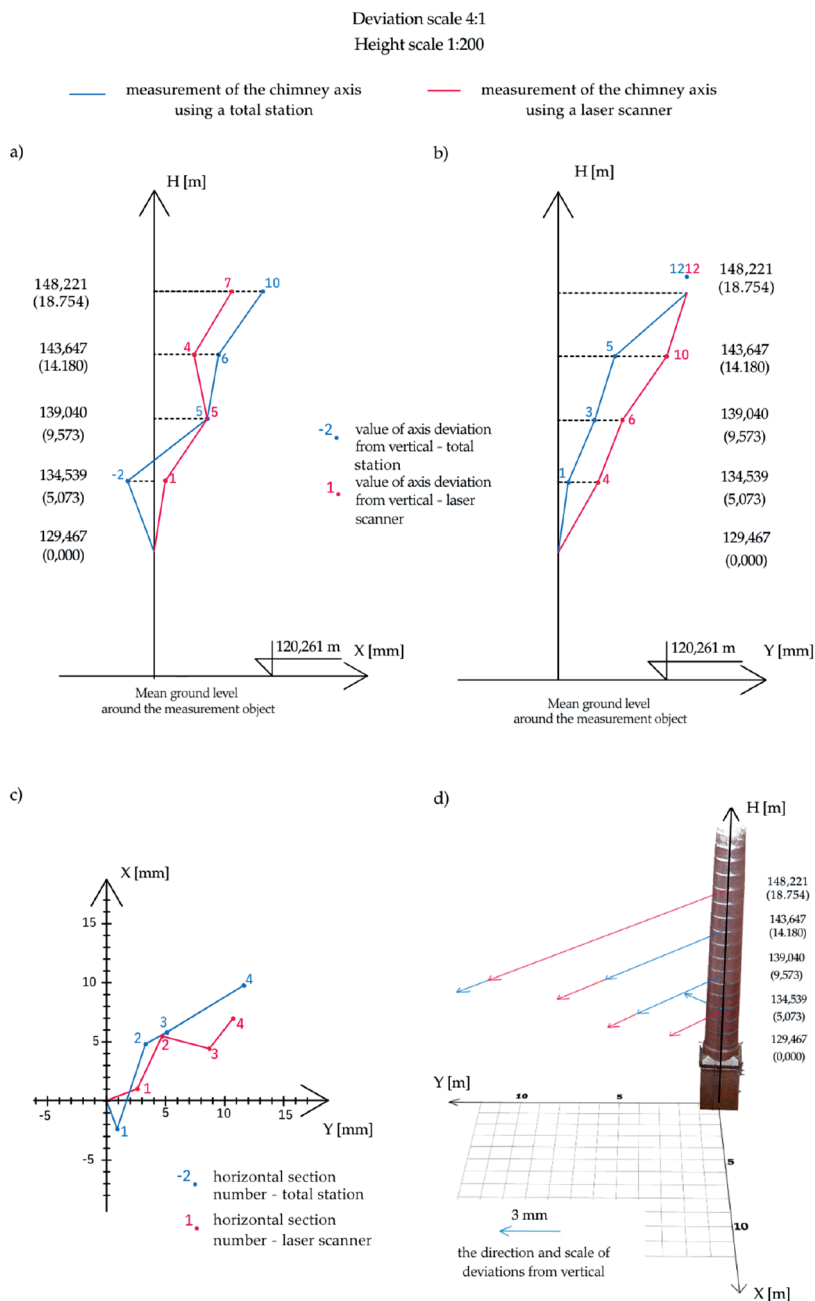
3. Results

Table 1 presents the chimney axis displacements at successive measurement levels relative to the reference level 0, determined by the surrounding tangents method, together with the mean elevations of the measurement levels and the corresponding chimney radii. Table 2 presents the chimney axis displacements obtained from terrestrial laser scanning, along with the RMS error of circle fitting.

Comparison of the chimney axis deviation results presented in both tables indicates consistency in the trend of increasing deviations with height. In both datasets, deviations along the Y axis increase more dynamically than along the X axis. The deviations in the X axis exhibit slightly less regularity, yet they also show an upward trend. The largest differences between the results obtained with the two methods are observed at level 4, where the discrepancy in the X axis is approximately 0.003 m and in the Y axis

Table 1. Reference results of chimney axis deviations determined by total station measurements with the surrounding tangents method

| Level | Deviation along the X-axis [m] | Deviation along the Y-axis [m] | M _o (unit weight standard deviation) | Average height [m] | Average height relative to level 0 [m] | Average radius [m] | Standard deviation of the radius [m] |
|-------|--------------------------------------|--------------------------------------|--|-----------------------|--|--------------------------|--|
| 0 | 0.0000 | 0.0000 | 1.0040 | 129.467 | 0.000 | 1.895 | 0.004 |
| 1 | -0.0024 | 0.0009 | 0.9215 | 134.539 | 5.073 | 1.830 | 0.003 |
| 2 | 0.0048 | 0.0033 | 0.9203 | 139.040 | 9.573 | 1.785 | 0.003 |
| 3 | 0.0058 | 0.0051 | 1.1041 | 143.647 | 14.180 | 1.720 | 0.001 |
| 4 | 0.0098 | 0.0116 | 0.7583 | 148.221 | 18.754 | 1.646 | 0.004 |
| 5 | 0.0071 | 0.0107 | 1.0145 | 152.920 | 23.454 | 1.546 | 0.002 |
| 6 | -0.0052 | 0.0256 | 1.0505 | 157.426 | 27.960 | 1.427 | 0.003 |
| 7 | 0.0017 | 0.0221 | 0.9551 | 161.765 | 32.299 | 1.330 | 0.005 |



Source: Authors' own study

Fig. 6. Graphical representation of chimney axis deviations: (a) deviations in the X direction, (b) deviations in the Y direction, (c) chimney axis deviations in the horizontal plane X-Y, (d) directions of deviations at individual chimney levels in the X, Y, H space

about 0.0004 m. At lower levels, the deviations are even more similar, with discrepancies within the range of 1–3 mm. Therefore, it can be concluded that the maximum differences between the methods do not exceed a few millimeters and do not significantly affect the overall pattern of chimney axis deviations increasing with height.

Table 2. Results of chimney axis deviations determined by TLS measurements using the circle fitting method

| Level | Deviation along the X-axis [m] | Deviation along the Y-axis [m] | RMS |
|-------|--------------------------------|--------------------------------|--------|
| 0 | 0.000 | 0.000 | 0.0042 |
| 1 | 0.001 | 0.004 | 0.0041 |
| 2 | 0.005 | 0.006 | 0.0058 |
| 3 | 0.004 | 0.010 | 0.0054 |
| 4 | 0.007 | 0.012 | 0.0056 |

Figure 6 presents a graphical representation of the chimney axis deviations in both directions (X, Y). The plots illustrate:

- deviations in the X direction (Fig. 6a),
- deviations in the Y direction (Fig. 6b),
- deviations of the chimney axis in the horizontal plane X-Y (Fig. 6c),
- directions of deviations at individual chimney levels in the X, Y, H space (Fig. 6d).

This visualization enables not only the analysis of absolute deviation values in particular directions but also the assessment of the overall trend of displacements and their spatial characteristics.

4. Discussion

The conducted study demonstrated that the use of the Leica BLK360 scanner, despite its technical limitations, allows for obtaining results comparable to total station measurements in the analysis of the verticality of tall structures. Of particular importance is the observed consistency in the trend of chimney axis deviations, obtained both using the method of enclosing tangents and through the analysis of the point cloud acquired from laser scanning. The discrepancies between the two methods, which did not exceed 5 mm, fall within acceptable measurement error margins, confirming the potential application of this class of equipment in geodetic tasks requiring higher accuracy.

The accuracy of deviation determination from the point cloud is significantly influenced by the method of geometric model fitting. In this study, the least squares method was used to fit circles to rings extracted from the point cloud. The obtained RMS values indicate a high quality of fitting. The density of the point cloud, achieved up to

the fifth measurement level, was sufficient to extract rings with widths not exceeding a few centimeters. Alternatively, robust estimation methods [Muszyński 2014] can be applied to reduce the influence of outliers. Moreover, in the case of wider rings, it may be appropriate to use a conical model, which better represents the actual geometry of an industrial chimney. Wider rings usually occur when the point cloud is sparse or when parts of the object's surface are partially obstructed, for example by ladders. In the analyzed object, neither the chimney nor its surroundings caused data obstruction, allowing the acquisition of a dense point cloud and the extraction of narrow rings. Under such conditions, the least squares method provided satisfactory fitting results. However, it should be noted that for taller industrial chimneys, with limited accessibility or partially obstructed by structural elements, the BLK360 scanner may prove insufficient.

At the same time, the limitations of the BLK360 scanner should be emphasized, particularly its relatively short measurement range, which is even smaller than declared by the manufacturer for vertical measurements. This is especially important for slender structures, where data must be acquired at multiple height levels. Difficulties in scanning dedicated target plates also limit the ability to precisely correlate and control the data. As indicated by Muszynski and Milczarek [2017], the quality of the point cloud – the most important measurement product – largely depends on structural accessibility and weather conditions. In our case, the weather conditions were ideal; however, under less favorable conditions, scan quality may be insufficient.

Despite these limitations, a significant advantage of the applied solution remains the speed of measurement, enabling more frequent monitoring of engineering structures. Even with limited accuracy, this facilitates early detection of potential geometric irregularities in the structure, which may form the basis for conducting more detailed total station measurements or using other high-precision methods.

The obtained results indicate that BLK360-class scanners can serve as a valuable supplement to conventional measurement methods for monitoring deformations in tall structures. Their main advantage is the ability to capture deformations across the entire surface, allowing for more frequent observations and the early detection of concerning trends in structural behavior, while more precise geodetic techniques – although limited to a few points – remain essential for the final verification of results. In future studies, it would be worthwhile to consider integrating scanning measurements with total station methods, in order to combine the advantages of both technologies and create a comprehensive system for monitoring verticality and deformations of engineering structures.

5. Conclusions

Based on the presented case study, the following conclusions can be drawn:

1. The measurements of the verticality of the industrial chimney showed consistency between the results obtained using total station and TLS, with maximum discrepancies not exceeding 5 mm.

2. The main advantage of the Leica BLK360 scanner is the speed and ease of data acquisition, enabling more frequent monitoring of structures and early detection of potential irregularities.
3. To validate the findings of this case study, the equipment should be tested on other structures.
4. Future studies should consider using larger target plates with better reflectivity and comparing the BLK360 with higher-end devices to evaluate its accuracy and effective range of use.
5. An important aspect for future investigation is the impact of atmospheric conditions and structural accessibility on data quality, along with the development of methods to compensate for these limitations.

In conclusion, the Leica BLK360 compact laser scanner can serve as a valuable supplement to conventional measurement methods in monitoring deformations of tall engineering structures, particularly in applications requiring frequent observations and rapid assessment of structural trends.

References

- Barazzetti L., Previtali M., Roncoroni F. 2019. The use of terrestrial laser scanning techniques to evaluate industrial masonry chimney verticality. *Int. Arch. Photogramm. Remote Sens. Spatial Inf. Sci.* XLII-2/W11, 173–178. DOI: 10.5194/isprs-archives-XLII-2-W11-173-2019
- Beshr A.A., Basha A.M., El-Madany S.A., El-Azeem F.A. 2023. Deformation of high rise cooling tower through projection of coordinates resulted from terrestrial laser scanner observations onto a vertical plane. *ISPRS Int. J. Geo-Inf.*, 12(10), 417. DOI: 10.3390/ijgi12100417
- Chmielewski T., Breuer P., Gorski P., Konopka E. 2009. Monitoring of tall slender structures by GPS measurements. *Wind & Structures*, 12(5), 401–412.
- Daliga K., Kurałowicz Z. 2019. Comparison of different measurement techniques as methodology for surveying and monitoring stainless steel chimneys. *Geosciences*, 9(10), 429. DOI:10.3390/geosciences9100429
- Gikas V. 2012. Ambient vibration monitoring of slender structures by microwave interferometer remote sensing. *J. Appl. Geod.*, 6(3–4). DOI:10.1515/jag-2012-0029
- Głowacki T. 2022. Monitoring the geometry of tall objects in energy industry. *Energies*, 15(7), 2324. DOI:10.3390/en15072324
- Marjetič A. 2018. TPS and TLS laser scanning for measuring the inclination of tall chimneys. *Geodetski Glasnik*, 49, 29–43. DOI:10.58817/2233-1786.2018.52.49.29
- Marjetič A., Štebe G. 2017. Determining the non-verticality of tall chimneys using the laser scanning approach. Faculty of Civil and Geodetic Engineering, University of Ljubljana.
- Matwij W., Lipecki T., Jaśkowski W.F. 2024. Selection of an algorithm for assessing the verticality of complex slender objects using semi-automatic point cloud analysis. *Remote Sens.*, 16(3), 435. DOI:10.3390/rs16030435
- Muszyński Z. 2014. Application of robust estimation methods to calculation of geometric distortions of a cooling tower shell. 14th Int. Multidiscip. Sci. GeoConf. SGEM, 65–72.
- Muszyński Z., Milczarek W. 2017. Application of terrestrial laser scanning to study the geometry of slender objects. *IOP Conf. Ser.: Earth Environ. Sci.*, 95, 042069. DOI: 10.1088/1755-1315/95/4/042069

- Owerko T., Ortyl L., Kocierz R., Kuras P. 2012. Novel technique of radar interferometry in dynamic control of tall slender structures. *Journal of Civil Engineering and Architecture*, 6(8), 1007.
- Pleterski Ž., Rak G., Kregar K. 2024. Determination of chimney non-verticality from TLS data using RANSAC method. *Remote Sens.*, 16(23), 4541. DOI:10.3390/rs16234541
- Popović J., Pandžić J., Pejić M., Vranić P., Milovanović B., Martinenko A. 2022. Quantifying tall structure tilting trend through TLS-based 3D parametric modelling. *Measurement*, 188, 110533. DOI:10.1016/j.measurement.2021.110533
- Siwiec J., Lenda G. 2022. Integration of terrestrial laser scanning and structure from motion for the assessment of industrial chimney geometry. *Measurement*, 199, 111404. DOI: 10.1016/j.measurement.2022.111404
- Teng J., Shi Y., Wang H., Wu J. 2022. Review on the research and applications of TLS in ground surface and constructions deformation monitoring. *Sensors*, 22(23), 9179. DOI: 10.3390/s22239179
- Zrinjski M., Tupek A., Barković Đ., Polović A. 2021. Industrial masonry chimney geometry analysis: a total station based evaluation of the unmanned aerial system photogrammetry approach. *Sensors*, 21(18), 6265. DOI:10.3390/s21186265